ACS OMEGA

http://pubs.acs.org/journal/acsodf

Article

Sustained Biochemical Signaling and Contact Guidance by Electrospun Bicomponents as Promising Scaffolds for Nerve Tissue Regeneration

Chaoyu Liu,[⊥] Zhiping Wang,[⊥] Xumei Yao, Min Wang, Zhigang Huang,* and Xiaohua Li*

Cite This: *ACS Omega* 2021, 6, 33010−33017

Read Online

ACCESS | Metrics & More | Article Recommendations

ABSTRACT: Electrospun fibers are excellent delivery vehicles enabling a sustained release of growth factors to elicit favorable cell responses and are increasingly used in tissue engineering. Scaffolds with specific physical/topographical features can also guide cell migration and maturation. Therefore, growth factor-loaded electrospun scaffolds with a designed topography are promising for tissue regeneration. In this investigation, aligned-fiber scaffolds composed of poly(lactic-*co*-glycolic acid) nanofibers incorporating a glial cell line-derived growth factor and poly (D,L-lactic acid) nanofibers incorporating a nerve growth factor were produced by electrospinning. The scaffolds provided an aligned fibrous topography and a dual release of growth factors. The rat pheochromocytoma cell (PC12 cell) response to produced non-woven and aligned-fiber scaffolds with/without growth factors was studied. The dual release of growth factors and topographical cues provided by aligned-fiber bicomponent scaffolds induced significant neurite extension, neuronal differentiation, and neurite alignment in a synergistic manner. The scaffolds with predesigned biochemical/topographical cues demonstrated in this study might be promising for nerve tissue repair.

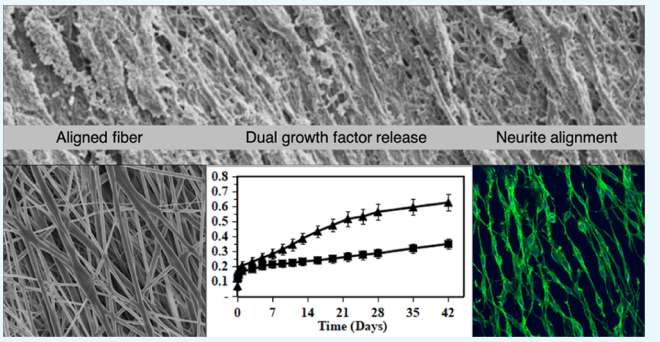

1. INTRODUCTION

Tissue engineering scaffolds are designed to recapitulate cell niche and/or provide required biochemical signals. To date, the investigations on the effects of topographical cues, biological cues, and electrochemical cues have gained increasing attention, suggesting that scaffolds with both biosignal capability and appropriate topographical features are promising in inducing the regeneration of targeted tissues.

In peripheral nerve tissue engineering, local and sustained delivery of growth factors from biodegradable scaffolds has promoted neural differentiation.[1−5] Biocompatible nerve conduits with designed topographical features have been used to provide native neuronal cells with contact guidance, promoting neuronal growth and axonal extension in different ways.[6−16] Among various fabrication techniques, electrospinning is advantageous in making extracellular matrix-like scaffolds with a designed pore size, porosity, fiber diameter, and alignment. Meanwhile, electrospun scaffolds are also efficient delivery vehicles of labile biomolecules.[17−22]

In this study, electrospun scaffolds with both aligned topographical guidance and dual release of growth factors were made, aiming at eliciting enhanced neurite outgrowth, neural differentiation, and neurite alignment. Fibrous bicomponent scaffolds with aligned fibers were fabricated through high-speed dual-source dual-power electrospinning (HS-DSDP-ES). Bicomponent scaffolds with a randomly orientated fibrous structure (non-woven scaffolds) were made as a control. The structure and morphology of scaffolds and the in vitro release of both growth factors were investigated. The rat pheochromocytoma cell line (PC12) was used for in vitro experiments. Neurite outgrowth, neural differentiation, and cell alignment on scaffolds were investigated and quantified using immunofluorescence staining.

2. RESULTS

2.1. Characterization of Scaffolds. Aligned-fiber scaffolds were made through HS-DSDP-ES, whereas non-woven scaffolds were made through normal DSDP-ES. Both types of fibers were uniformly distributed in aligned-fiber scaffolds, showing a distinct fiber alignment (Figure 1a). It can be seen

Received: September 15, 2021
Accepted: November 15, 2021
Published: November 24, 2021

https://doi.org/10.1021/acsomega.1c05117
ACS Omega 2021, 6, 33010−33017

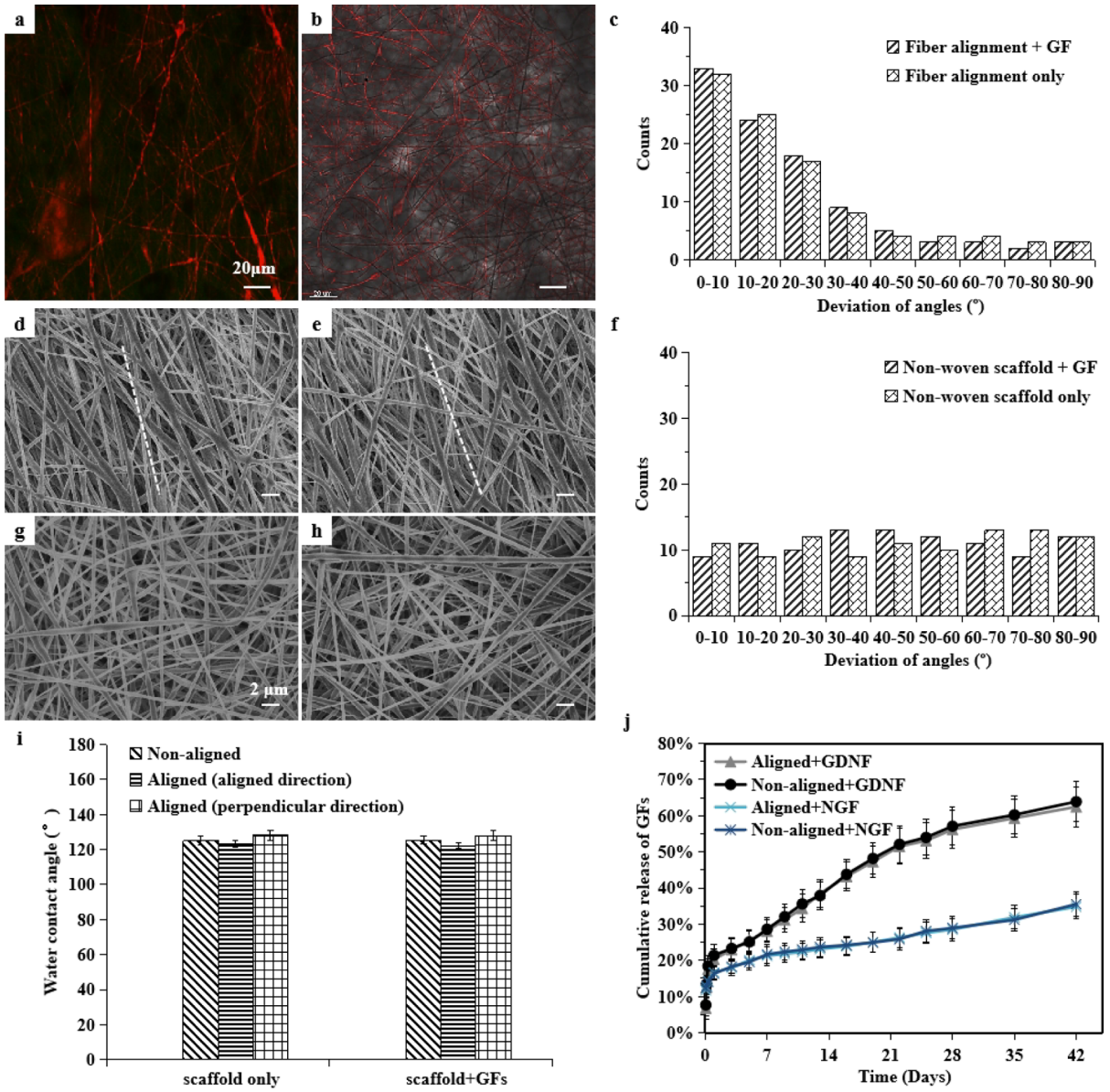

Figure 1. Confocal image of aligned-fiber (a) and non-woven (b) bicomponent scaffolds containing rhodamine-B-labeled nerve growth factor (NGF)/poly (D,L-lactic acid) (PDLLA) fibers. SEM image of aligned-fiber + GFs (d), aligned-fiber only (e), non-aligned fiber + GFs (g), and non-aligned fiber only (h) scaffolds. Distribution of fiber orientations in aligned-fiber (c) and non-woven (f) bicomponent scaffolds. Water contact angles (i) and GF release profile (j) of the fibrous bicomponent scaffold.

that fibers had similar average fiber diameters (around 500 nm) in all scaffolds. The fiber alignment was clearly visible in aligned-fiber scaffolds (Figure 1d,e), while a non-woven fibrous structure was seen in non-woven scaffolds (Figure 1g,h). The distribution of fiber orientations in aligned-fiber scaffolds and non-woven scaffolds is shown in Figure 1c,f. A narrow distribution of fiber orientations was observed in aligned-fiber scaffolds, indicating a high fiber alignment. By contrast, a wide distribution of fiber orientations was found in non-woven scaffolds, which indicated a low fiber alignment.

The wettability of produced scaffolds was measured by water contact angle (WCA) tests. The WCAs of aligned-fiber bicomponent scaffolds in different directions were examined. As shown in Figure 1l, the WCA was 122.3 ± 1.3 and 127.9 ± 3.0° in the aligned direction and the perpendicular direction, respectively.

2.2. In Vitro Release of Growth Factors. The release behavior of both growth factors from scaffolds was investigated. A fast glial cell line-derived growth factor (GDNF) release and a slower NGF release are shown in Figure 1j. 16.7% of NGF was released in initial 24 h and up to 34.8% of NGF was released after 42 days. During the initial release period (24 h), 20.3% of GDNF was released, and 62.5% GDNF release was achieved after 42 days. The results showed that sustained and dual release of growth factors with different release behaviors was achieved.

2.3. Cell Morphology. PC12 cells were cultured on scaffolds and their morphology is shown in Figure 2. In general, cell adhesion, spreading, and migration on all types of scaffolds were improved with increasing culture time.

At day 1, cells on non-woven scaffolds without growth factors (Figure 2b) were in spherical shape with little spreading. Cells on growth factor-containing non-woven

https://doi.org/10.1021/acsomega.1c05117
ACS Omega 2021, 6, 33010−33017

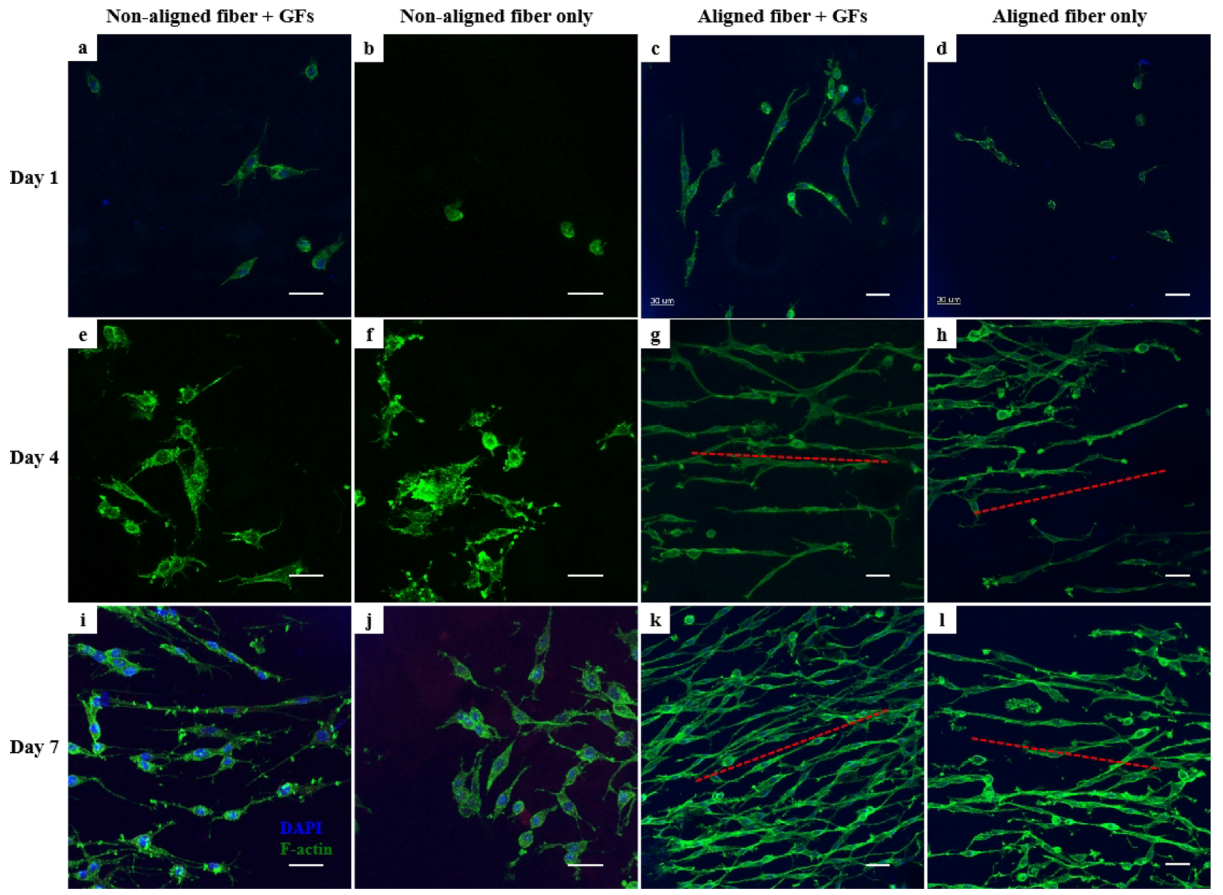

Figure 2. Confocal micrographs of PC12 cells grown on scaffolds: non-aligned fiber + GFs (a,e,i), non-aligned fiber only (b,f,j), aligned fiber + GFs (c,g,k), and aligned fiber only (d,h,l) at days 1, 4, and 7, respectively. Scale bar: 30 μm.

scaffolds (Figure 2a) exhibited improved cell attachment, spreading, and migration. After 4 days of culture, more cells were elongated to an elliptical shape, and improved neurite extensions were observed on scaffolds with GFs (Figure 2e) as compared to those without GFs. The neurite sprouts on both non-woven scaffolds protruded in random orientations. Most cells showed an elongated elliptical shape on aligned-fiber scaffolds in spite of no growth factor stimulation (Figure 2h). Much improved neurite sprouting and elongation was also seen on the aligned-fiber scaffolds as compared to the cell morphology on non-woven fibrous scaffolds without growth factors. Some of the neurite protrusions showed an alignment in the direction of the red-dotted line (Figure 2g). After 7 days of culture, cells on growth factor-containing non-woven scaffolds (Figure 2i) showed improved neurite branching and neurite outgrowth. Neurite branching and outgrowth protruded in random orientations on both types of non-woven scaffolds. Cells on aligned-fiber scaffolds appeared to spread in a well-organized manner. Much increased neurite sprouting and elongation was also seen on the aligned-fiber scaffolds as compared to the cell morphology on non-woven fibrous scaffolds without growth factors. The neurite alignment was obviously seen as revealed by the read-dotted line.

2.4. Analysis of Neurite Differentiation. Neurite differentiation and alignment were characterized as shown in Figure 3. At day 1, cell differentiation in the GF-containing group was higher than that in the control group. More cell differentiation was obtained in the aligned-fiber group compared with the non-woven group. The results showed limited neurite differentiation was induced at day 1. At day 4, cell differentiation in the GF-containing group was much higher than that in the control group. More cell differentiation was obtained in the aligned-fiber group compared with the non-woven group. The longest neurite outgrowth was achieved on GF-containing aligned-fiber scaffolds. At day 7, much higher cell differentiation percentage was obtained in the GF-containing group compared with the control group. More cell differentiation was achieved in the aligned-fiber group compared with the non-woven group. Significant neurite extensions were obtained on both aligned-fiber scaffolds without GFs and GF-containing non-woven scaffolds. A random distribution of neurite orientations was found in non-woven fibrous scaffolds (Figure 3d). However, a highly organized arrangement of neurite orientations was noticed in both types of aligned-fiber scaffolds (Figure 3c), indicating that a good neurite alignment was achieved attributed to the fiber alignment.

2.5. Cell Morphology on Scaffolds. SEM images of cells grown on scaffolds are shown in Figure 4. Enhanced cell attachment, spreading, and migration over culture time were observed. Cells proliferated well on fibrous scaffolds and covered a large portion of the scaffold surfaces at day 7. Cell differentiation characterized by neurite outgrowth on fibrous scaffolds increased over culture time as more cells being in the elongated elliptical shape with neurite protrusions were seen at day 4 and day 7. The stimulation of GFs released from fibrous scaffolds significantly improved cell differentiation in both non-woven scaffolds and aligned-fiber scaffolds as more cells in the

https://doi.org/10.1021/acsomega.1c05117
ACS Omega 2021, 6, 33010−33017

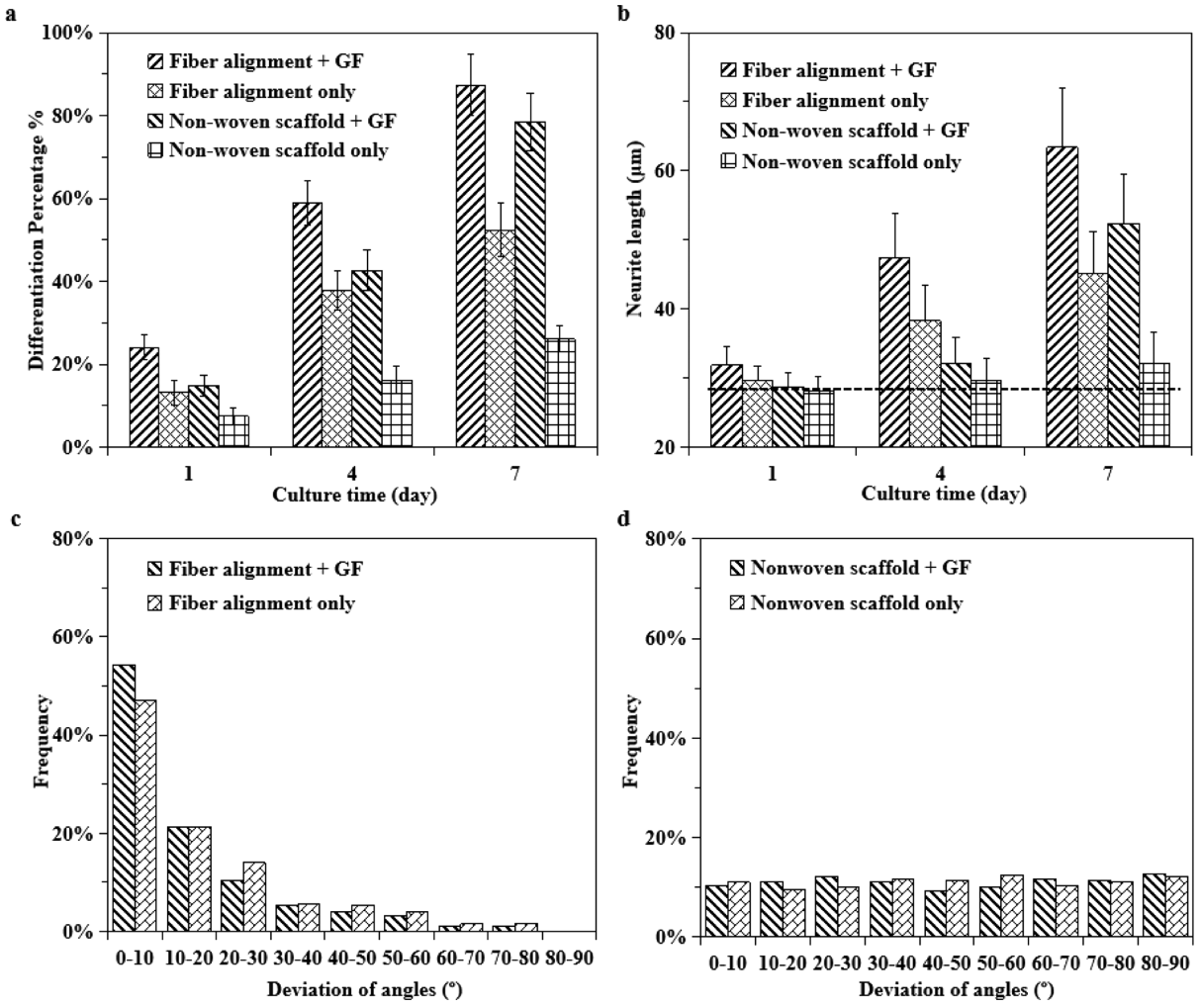

Figure 3. Differentiation percentages of PC12 cells grown on scaffolds (a). Neurite length (dotted line: 28 μm) (b). Distribution of neurite orientations on aligned-fiber scaffolds (c) and non-woven scaffolds (d).

elliptical shape bearing neurite outgrowth but less cells in the spherical shape were clearly seen on GF-containing scaffolds as compared to scaffolds without GFs. The fiber alignment also contributed to the elongation of cells, neurite outgrowth, and neural differentiation. High-resolution SEM micrographs (insets in Figure 4g,h,k,l) revealed more details about neurite outgrowth and cell−scaffold interactions on aligned-fiber scaffolds. It was found that neurite protrusions tended to extend along fibers underneath and appreciable amounts of short filopodia and microspikes protruded out of the cell body toward adjacent fibers. The fiber alignment noticeably increased cell differentiation as much more neurite outgrowth was observed on aligned-fiber scaffolds compared with non-woven fibrous scaffolds. These results showed that the fiber alignment in fibrous scaffolds and released GFs promoted neurite outgrowth and neural differentiation independently or synergistically.

3. DISCUSSION

Scaffold-based nerve guidance conduits mimicking the micro-environments are important for peripheral nerve regeneration. Studies have shown that plain nanostructured scaffolds can provide topographical cues to enhance neurite outgrowth. Neuronal growth and axonal extension can also be promoted by neurotrophic factors secreted from surrounding.[4] Due to the vulnerability and short half-lives of these growth factors, delivery vehicles are essential for their controlled release.[23,24] Therefore, the combination of sustained delivery of dual growth factors (GDNF and NGF) and topographical signaling to seeded cells within a single scaffold would be advantageous.

Biocompatible scaffolds resembling natural ECM can induce enhanced cell adhesion, migration, and proliferation.[25−28] Electrospun fibers have been employed to deliver various bioactive molecules including proteins and nucleic acids.[21−23,29−31] In this study, scaffolds with dual growth factor delivery and an aligned-fibrous structure were produced, attempting to provide biochemical cues and topographical cues simultaneously for enhanced neurite outgrowth, differentiation, and neurite alignment.

Topographical signaling plays important roles in cell sensing, focal adhesions, cell contractility, and other cell activities.[32,33] It was reported that neuronal differentiation and neurite alignment of PC12 cells could be achieved on various nanogratings with or without the stimulation of biochemical cues.[6,8,10] Highly aligned electrospun fibers could guide neurite outgrowth along fibers.[34] It was also claimed that the fiber diameter could influence the cellular response and determine cell fate.[35,36] Aligned fibers could be produced through a high-speed electrospinning (HS-ES) technique, which could help alleviate or eliminate bending instability of electrospun fibers

https://doi.org/10.1021/acsomega.1c05117
ACS Omega 2021, 6, 33010−33017

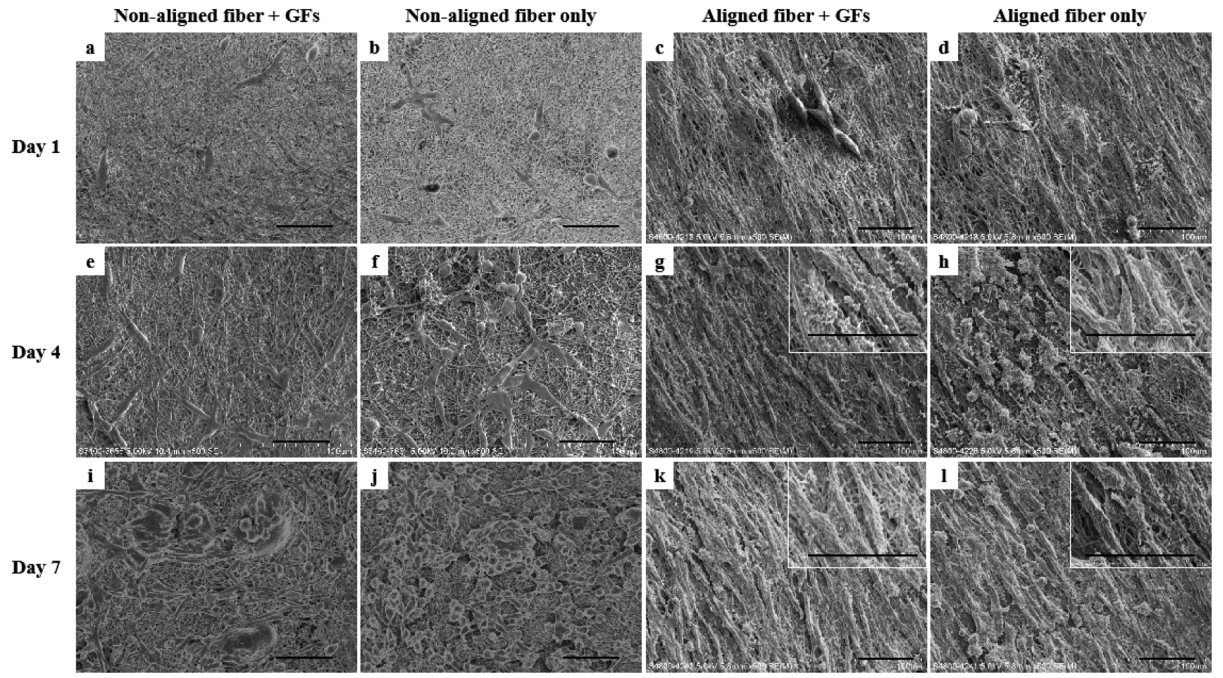

Figure 4. SEM images of PC12 cells grown on scaffolds: non-aligned fiber + GFs (a,e,i), non-aligned fiber only (b,f,j), aligned fiber + GFs (c,g,k), and aligned fiber only (d,h,l). Scale bar: 50 μm.

and consequently facilitate fiber alignment.[37,38] The fiber alignment would decrease with the increase of the scaffold thickness.[39,40] Fibrous bicomponent scaffolds with aligned-fiber structures and an even distribution of both types of fibers were achieved here through the HS-DSDP-ES.

It is well known that wettability of scaffolds would influence cell spreading and adhesion. The wettability of produced aligned-fiber bicomponent scaffolds in different directions was both above 120° (Figure 1i), revealing that the produced fibrous scaffold was hydrophobic. The wettability of bicomponent scaffolds was predominantly influenced by the PDLLA component, which was consistent with the study reported by other groups.[41] In wettability tests, the static contact angle in the x-direction (aligned direction of fibers) was defined as θ_x and the static contact angle in the y-direction (perpendicular direction to the fiber alignment) was defined as θ_y. Wetting anisotropy was defined as $\Delta\theta = \theta_y - \theta_x$. In this study, θ_y was 127.9°, θ_x was 122.3°, and $\Delta\theta$ was 5.6°. The anisotropy was caused by preferential spreading and ingression of water droplets in the x-direction.[42]

Dual release of growth factors with different release profiles was achieved in this investigation. NGF and GDNF can both stimulate neurite outgrowth and neural differentiation through a specific signaling pathway.[3,43] In our recent study, it was found that dual delivery of NGF and GDNF could promote neurite outgrowth and neural differentiation synergistically.[31]

Contact guidance provided by aligned fibers induced a much higher level of neurite outgrowth and neuronal differentiation and an obvious neurite alignment (Figure 2d,h,l) as compared to non-woven fibrous scaffolds (Figure 2b,f,j). Interestingly, cells on randomly oriented fibrous scaffolds showed partial neurite outgrowth and neuronal differentiation but no neurite alignment over the culture time, indicating that cells also responded to topographical cues provided by randomly oriented fibers. The neurite outgrowth and neuronal differentiation might be attributed to short-ranged topographical guidance. The long-ranged topographical guidance was disturbed by randomly oriented fibers and resulted in no neurite alignment. The neurite outgrowth on fibrous scaffolds and cell-scaffold interactions were revealed by SEM micrographs.

Elongated cells with an elliptical shape on fibrous scaffolds differentiated as characterized by neurite outgrowth tending to extend along fibers underneath. The observations might be explained by the involvement of focal adhesions, which coordinate cell polarity and cytoskeleton arrangement and consequently motivate neurite migration and path-finding.[44,45] In this study, the difficulty in establishing focal adhesions to adjacent fibers resulted in cytoskeleton organization and cell migration preferentially along electrospun fibers underneath, which consequently led to cell polarity and neurite path-finding. The difficulty in establishment of focal adhesions to adjacent fibers was revealed by high-resolution SEM micrographs (insets in Figure 4g,h,k,l). Appreciable amounts of very short filopodia and microspikes protrude out of the cell body toward adjacent fibers in the orthogonal direction of the fiber alignment but most of them failed to anchor to the adjacent fibers. Therefore, a much higher level of neurite outgrowth and neuronal differentiation and more obvious neurite alignment were observed in aligned-fiber scaffolds.

Interestingly, the degree of neurite alignment was significantly higher than that of the fiber alignment, suggesting that the neurite alignment was tolerant of topographical noise to a certain extent. The degree of neurite alignment in GF-containing aligned-fiber scaffolds was slightly higher than that in the aligned-fiber scaffolds without growth factors, indicating that growth factors contributed to the neurite alignment synergistically in the context of topographical guidance.

It can be concluded that growth factors released from scaffolds and topographical cues induced enhanced neurite outgrowth and differentiation in different manners. With the combinatory stimulation of biochemical cues and topo-

https://doi.org/10.1021/acsomega.1c05117
ACS Omega 2021, 6, 33010−33017

graphical cues, most neuronal differentiation and neurite alignment was achieved. Although these results highlighted the effectiveness of aligned bicomponent fibrous scaffolds in guiding neurite outgrowth, neuronal differentiation, and neurite alignment, the non-human cell line used in this study has a limited translational value for nerve conduit application. More representative human neural cells should be utilized in the future investigation of nerve tissue regeneration.

4. CONCLUSIONS

Fibrous bicomponent scaffolds providing both biochemical cues and contact guidance were fabricated through HS-DSDP-ES. The dual delivery of GDNF and NGF and the topographical cues in aligned bicomponent scaffolds induced significant neurite extension, neuronal differentiation, and neurite alignment in a synergistic manner. The elaborately designed scaffolds providing multiple microenvironmental signals in a controlled manner are promising for potential applications.

5. EXPERIMENTAL SECTION

5.1. Materials. Poly(lactic-*co*-glycolic acid) (PLGA, LA/GA = 50:50, M_w = 100 kDa) and PDLLA (M_w = 100 kDa) were supplied by Lakeshore Biomaterials. The human β-NGF with the ELISA kit was supplied by Peprotech Inc., and human GDNF with the ELISA kit was supplied by R&D Systems, Inc. The culture medium and other reagents were purchased from Invitrogen, Inc. All chemicals were used as purchased.

5.2. Fabrication of Electrospun Scaffolds. NGF or GDNF containing DI water (supplemented with 0.5% BSA) and 5 wt % Span-80 were mixed with PLGA/chloroform or PDLLA/chloroform polymer solutions (15%, w/v) at a volume ratio of 10:1 for 10 min at 300 rpm to prepare water-in-oil (w/o) emulsions. The applied voltage during electrospinning was set at 16 kV. A needle tip with a 0.8 mm inner diameter was used. The needle-to-collector distance was optimized at 8 cm, and the feeding rate of emulsions was set at 2 mL/h. A drum collector rotating at 3000 rpm was used to make aligned-fiber scaffolds. The emulsion formula is shown in Table 1. The fabricated scaffolds were freeze-dried for 24 h.

Table 1. Emulsion Formula

	GDNF/PLGA emulsions		NGF/PDLLA emulsions	
scaffold	water phase[a]	oil phase[b]	water phase[a]	oil phase[b]
aligned-fiber scaffolds + GFs	GDNF	PLGA	NGF	PDLLA
aligned-fiber scaffolds	NA	PLGA	NA	PDLLA
non-woven scaffolds + GFs	GDNF	PLGA	NGF	PDLLA
non-woven scaffolds	NA	PLGA	NA	PDLLA

[a]5 μg of growth factors was added to the water phase (1 mL H_2O). [b]The oil phase was formed by dissolving 1.5 g of polymers in 10 mL $CHCl_3$.

5.3. Characterization. Produced scaffolds were processed using a sputter coater (BEL-TACSCD005) and examined under a scanning electron microscope (Hitachi S-4800 FEG, Japan). WCAs of scaffolds at room temperature were examined using a measuring machine (Solon SL200B, China).

5.4. In Vitro Release Tests. For in vitro release tests, previous procedures were followed.[46] PBS release medium containing 0.5% BSA, 0.1% heparin, 0.05% Tween-20, and 0.02% NaN_3 was prepared. 50 mg freeze-dried scaffolds were immersed in 3 mL release medium and incubated in a 37 °C water bath. About 0.4 mL release medium was collected and replaced by 0.4 mL fresh release medium at different times during the 42 day tests. The concentration of growth factors in the collected release medium was measured by ELISA.

5.5. In Vitro Experiments. PC12 cells (Biowit, China) were maintained and expanded in DMEM medium and incubated in a 5% CO_2 atmosphere at 37 °C. The culture medium was replaced every 2 days. When the cultured cells reached 80% confluence, they were used for further experiments.

5.6. Cell Adhesion and Proliferation. Scaffold samples (5 mg each) in the square shape were sterilized by ^{60}Co γ-irradiation at a dose of 15 kGy before any further experiment. Samples were immersed in the culture medium and fixed at the bottom of the culture plate. About 4×10^3 PC12 cells were seeded on each scaffold. After preset culture times, the cell-scaffold constructs were collected and washed two times with PBS, followed by 10 min fixation with 4% PFA at room temperature. After that, cells were treated with 0.1% Triton X-100 in (1% w/v) BSA block solution for 30 min. The cytoskeletons and nuclei of cells were stained with FITC phalloidin (1:40 dilution) for 30 min and DAPI (1:1000 dilution) for 5 min. Cells were observed using a confocal laser scanning microscope (CLSM 710, Carl Zeiss).

The samples with cells were rinsed with PBS and fixed with 2.5% glutaraldehyde at 4 °C for 4 h, followed by further washing with 0.1 M sucrose-containing sodium cacodylate buffer, PBS, and DI water. The cell-scaffold samples were further freeze-dried for 48 h, sputter-coated with gold, and photographed using a scanning electron microscope.

5.7. Image Analysis. Image J software (NIH, USA) was used for morphological analysis. SEM micrographs and confocal images were loaded into Image J to measure the fiber alignment, neurite length, and neural orientation. Outgrowth of cells longer than 28 μm were counted as neurites. At least 100 fibers or cells in each scaffold were randomly selected for measuring the fiber alignment, neurite length, and neural orientation.

5.8. Statistical Analysis. All of the data were achieved at least in triplicate, and the results were expressed as the mean and standard deviation.

AUTHOR INFORMATION

Corresponding Authors

Zhigang Huang − *Department of General Practice, Peking University Shenzhen Hospital, Shenzhen 518036, China*; Email: dochzg@163.com

Xiaohua Li − *Department of Research and Development, Shenzhen Shiningbiotek Company Limited, Shenzhen 518055, China*; Email: lxh@shiningbiotek.com

Authors

Chaoyu Liu − *Department of Research and Development, Shenzhen Shiningbiotek Company Limited, Shenzhen 518055, China*

Zhiping Wang − *Department of Research and Development, Shenzhen Anlv Medical Technology Company Limited, Shenzhen 518055, China*

https://doi.org/10.1021/acsomega.1c05117
ACS Omega 2021, 6, 33010−33017

Xumei Yao − *Department of Research and Development, Shenzhen Shiningbiotek Company Limited, Shenzhen 518055, China;* orcid.org/0000-0002-5577-3065
Min Wang − *Department of Mechanical Engineering, The University of Hong Kong, Hong Kong 999077, China*

Complete contact information is available at: https://pubs.acs.org/10.1021/acsomega.1c05117

Author Contributions

⊥C.L. and Z.W. contributed equally. All authors contributed to this paper and agreed to publish this final version.

Notes

The authors declare no competing financial interest.

■ ACKNOWLEDGMENTS

This research was supported by Hong Kong Research Grants Council (no. HKU718109E) and Guangdong Special Support Plan of China (no. 2015TQ01R546).

■ REFERENCES

(1) Catrina, S.; Gander, B.; Madduri, S. Nerve conduit scaffolds for discrete delivery of two neurotrophic factors. *Eur. J. Pharm.* **2013**, *85*, 139−142.
(2) Chung, J. H.; Kubota, H.; Ozaki, Y.; Uda, S.; Kuroda, S. Timing-Dependent Actions of NGF Required for Cell Differentiation. *PLoS One* **2010**, *5*, No. e9011.
(3) Madduri, S.; Papaloïzos, M.; Gander, B. Synergistic effect of GDNF and NGF on axonal branching and elongation in vitro. *Neurosci. Res.* **2009**, *65*, 88−97.
(4) Price, T. J.; Louria, M. D.; Candelario-Soto, D.; Dussor, G. O.; Jeske, N. A.; Patwardhan, A. M.; Diogenes, A.; Trott, A. A.; Hargreaves, K. M.; Flores, C. M. Treatment of trigeminal ganglion neurons in vitro with NGF, GDNF or BDNF: effects on neuronal survival, neurochemical properties and TRPV1-mediated neuropeptide secretion. *BMC Neurosci.* **2005**, *6*, 4.
(5) Porzionato, A.; Barbon, S.; Stocco, E.; Dalzoppo, D.; Contran, M.; De Rose, E.; Parnigotto, P. P.; Macchi, V.; Grandi, C.; De Caro, R. Development of Oxidized Polyvinyl Alcohol-Based Nerve Conduits Coupled with the Ciliary Neurotrophic Factor. *Materials* **2019**, *12*, 1996.
(6) Cecchini, M.; Bumma, G.; Serresi, M.; Beltram, F. PC12 differentiation on biopolymer nanostructures. *Nanotechnology* **2007**, *18*, 505103.
(7) Chew, S. Y.; Mi, R.; Hoke, A.; Leong, K. W. Aligned protein-polymer composite fibers enhance nerve regeneration: A potential tissue-engineering platform. *Adv. Funct. Mater.* **2007**, *17*, 1288−1296.
(8) Ferrari, A.; Faraci, P.; Cecchini, M.; Beltram, F. The effect of alternative neuronal differentiation pathways on PC12 cell adhesion and neurite alignment to nanogratings. *Biomaterials* **2010**, *31*, 2565−2573.
(9) Jenkins, P. M.; Laughter, M. R.; Lee, D. J.; Lee, Y. M.; Freed, C. R.; Park, D. A nerve guidance conduit with topographical and biochemical cues: potential application using human neural stem cells. *Nanoscale Res. Lett.* **2015**, *10*, 972.
(10) Tonazzini, I.; Meucci, S.; Faraci, P.; Beltram, F.; Cecchini, M. Neuronal differentiation on anisotropic substrates and the influence of nanotopographical noise on neurite contact guidance. *Biomaterials* **2013**, *34*, 6027−6036.
(11) Vijayavenkataraman, S. Nerve guide conduits for peripheral nerve injury repair: A review on design, materials and fabrication methods. *Acta Biomater.* **2020**, *106*, 54−69.
(12) Zhang, J.; Zhang, X.; Wang, C.; Li, F.; Qiao, Z.; Zeng, L.; Wang, Z.; Liu, H.; Ding, J.; Yang, H. Conductive composite fiber with optimized alignment guides neural regeneration under electrical stimulation. *Adv. Healthcare Mater.* **2021**, *10*, 2000604.
(13) Vashisth, P.; Kar, N.; Gupta, D.; Bellare, J. R. Three dimensional quercetin-functionalized patterned scaffold: development, characterization, and in vitro assessment for neural tissue engineering. *ACS Omega* **2020**, *5*, 22325−22334.
(14) Carvalho, C. R.; Oliveira, J. M.; Reis, R. L. Modern trends for peripheral nerve repair and regeneration: beyond the hollow nerve guidance conduit. *Front. Bioeng. Biotechnol.* **2019**, *7*, 337.
(15) Vijayavenkataraman, S.; Zhang, S.; Thaharah, S.; Sriram, G.; Lu, W. F.; Fuh, J. Y. H. Electrohydrodynamic jet 3D printed nerve guide conduits (NGCs) for peripheral nerve injury repair. *Polymers* **2018**, *10*, 753.
(16) Carvalho, C. R.; Wrobel, S.; Meyer, C.; Brandenberger, C.; Cengiz, I. F.; López-Cebral, R.; Silva-Correia, J.; Ronchi, G.; Reis, R. L.; Grothe, C.; et al. Gellan gum-based luminal fillers for peripheral nerve regeneration: an in vivo study in the rat sciatic nerve repair model. *Biomater. Sci.* **2018**, *6*, 1059−1075.
(17) Li, D.; Tao, L.; Shen, Y.; Sun, B.; Xie, X.; Ke, Q.; Mo, X.; Deng, B. Fabrication of multilayered nanofiber scaffolds with a highly aligned nanofiber yarn for anisotropic tissue regeneration. *ACS Omega* **2020**, *5*, 24340−24350.
(18) Wang, L.; Wu, Y.; Hu, T.; Ma, P. X.; Guo, B. Aligned conductive core-shell biomimetic scaffolds based on nanofiber yarns/hydrogel for enhanced 3D neurite outgrowth alignment and elongation. *Acta Biomater.* **2019**, *96*, 175−187.
(19) Jiang, X.; Cao, H. Q.; Shi, L. Y.; Ng, S. Y.; Stanton, L. W.; Chew, S. Y. Nanofiber topography and sustained biochemical signaling enhance human mesenchymal stem cell neural commitment. *Acta Biomater.* **2012**, *8*, 1290−1302.
(20) Puhl, S.; Ilko, D.; Li, L.; Holzgrabe, U.; Meinel, L.; Germershaus, O. Protein release from electrospun nonwovens: Improving the release characteristics through rational combination of polyester blend matrices with polidocanol. *Int. J. Pharm.* **2014**, *477*, 273−281.
(21) Wang, X.; Yuan, Y.; Huang, X.; Yue, T. Controlled release of protein from core-shell nanofibers prepared by emulsion electrospinning based on green chemical. *J. Appl. Polym. Sci.* **2015**, *132*, 41811.
(22) Yau, W. W. Y.; Long, H.; Gauthier, N. C.; Chan, J. K. Y.; Chew, S. Y. The effects of nanofiber diameter and orientation on siRNA uptake and gene silencing. *Biomaterials* **2015**, *37*, 94−106.
(23) Fischer, J.; Kolk, A.; Wolfart, S.; Pautke, C.; Warnke, P. H.; Plank, C.; Smeets, R. Future of local bone regeneration - Protein versus gene therapy. *J. Craniomaxillofac. Surg.* **2011**, *39*, 54−64.
(24) Roam, J. L.; Nguyen, P. K.; Elbert, D. L. Controlled release and gradient formation of human glial-cell derived neurotrophic factor from heparinated poly(ethylene glycol) microsphere-based scaffolds. *Biomaterials* **2014**, *35*, 6473−6481.
(25) Kharaziha, M.; Nikkhah, M.; Shin, S.-R.; Annabi, N.; Masoumi, N.; Gaharwar, A. K.; Camci-Unal, G.; Khademhosseini, A. PGS:Gelatin nanofibrous scaffolds with tunable mechanical and structural properties for engineering cardiac tissues. *Biomaterials* **2013**, *34*, 6355−6366.
(26) Nista, S. V. G.; Bettini, J.; Mei, L. H. I. Coaxial nanofibers of chitosan-alginate-PEO polycomplex obtained by electrospinning. *Carbohydr. Polym.* **2015**, *127*, 222−228.
(27) Park, S. Y.; Ki, C. S.; Park, Y. H.; Lee, K. G.; Kang, S. W.; Kweon, H. Y.; Kim, H. J. Functional recovery guided by an electrospun silk fibroin conduit after sciatic nerve injury in rats. *J. Tissue Eng. Regener. Med.* **2015**, *9*, 66−76.
(28) Xue, J.; He, M.; Liu, H.; Niu, Y.; Crawford, A.; Coates, P. D.; Chen, D.; Shi, R.; Zhang, L. Drug loaded homogeneous electrospun PCL/gelatin hybrid nanofiber structures for anti-infective tissue regeneration membranes. *Biomaterials* **2014**, *35*, 9395−9405.
(29) Llorens, E.; Ibañez, H.; Del Valle, L. J.; Puiggalí, J. Biocompatibility and drug release behavior of scaffolds prepared by coaxial electrospinning of poly(butylene succinate) and polyethylene glycol. *Mater. Sci. Eng., C* **2015**, *49*, 472−484.
(30) Liu, C.; Wang, C.; Zhao, Q.; Li, X.; Xu, F.; Yao, X.; Wang, M. Incorporation and release of dual growth factors for nerve tissue

engineering using nanofibrous bicomponent scaffolds. *Biomed. Mater.* **2018**, *13*, 044107.
(31) Liu, C.; Li, X.; Zhao, Q.; Xie, Y.; Yao, X.; Wang, M.; Cao, F. Nanofibrous bicomponent scaffolds for the dual delivery of NGF and GDNF: controlled release of growth factors and their biological effects. *J. Mater. Sci.: Mater. Med.* **2021**, *32*, 9.
(32) Biggs, M. J. P.; Richards, R. G.; Dalby, M. J. Nanotopographical modification: a regulator of cellular function through focal adhesions. *Nanomedicine* **2010**, *6*, 619−633.
(33) Geiger, B.; Spatz, J. P.; Bershadsky, A. D. Environmental sensing through focal adhesions. *Nat. Rev. Mol. Cell Biol.* **2009**, *10*, 21−33.
(34) Wang, H. B.; Mullins, M. E.; Cregg, J. M.; Hurtado, A.; Oudega, M.; Trombley, M. T.; Gilbert, R. J. Creation of highly aligned electrospun poly-L-lactic acid fibers for nerve regeneration applications. *J. Neural. Eng.* **2009**, *6*, 016001.
(35) Bashur, C. A.; Shaffer, R. D.; Dahlgren, L. A.; Guelcher, S. A.; Goldstein, A. S. Effect of fiber diameter and alignment of electrospun polyurethane meshes on mesenchymal progenitor cells. *Tissue Eng., Part A* **2009**, *15*, 2435−2445.
(36) Christopherson, G. T.; Song, H.; Mao, H.-Q. The influence of fiber diameter of electrospun substrates on neural stem cell differentiation and proliferation. *Biomaterials* **2009**, *30*, 556−564.
(37) Dabirian, F.; Hosseini Ravandi, S. A.; Pishevar, A. R.; Abuzade, R. A. A comparative study of jet formation and nanofiber alignment in electrospinning and electrocentrifugal spinning systems. *J. Electrost.* **2011**, *69*, 540−546.
(38) Liu, C.; Li, X.; Xu, F.; Cong, H.; Li, Z.; Song, Y.; Wang, M. Spatio-temporal release of NGF and GDNF from multi-layered nanofibrous bicomponent electrospun scaffolds. *J. Mater. Sci.: Mater. Med.* **2018**, *29*, 102.
(39) Theron, A.; Zussman, E.; Yarin, A. L. Electrostatic field-assisted alignment of electrospun nanofibres. *Nanotechnology* **2001**, *12*, 384.
(40) Tong, H.-W.; Wang, M. An Investigation into the Influence of Electrospinning Parameters on the Diameter and Alignment of Poly(hydroxybutyrate-co-hydroxyvalerate) Fibers. *J. Appl. Polym. Sci.* **2011**, *120*, 1694−1706.
(41) Chen, Z.; Cao, L.; Wang, L.; Zhu, H.; Jiang, H. Effect of fiber structure on the properties of the electrospun hybrid membranes composed of poly(ε-caprolactone) and gelatin. *J. Appl. Polym. Sci.* **2013**, *127*, 4225−4232.
(42) Wu, H.; Zhang, R.; Sun, Y.; Lin, D.; Sun, Z.; Pan, W.; Downs, P. Biomimetic nanofiber patterns with controlled wettability. *Soft Matter* **2008**, *4*, 2429−2433.
(43) Vaudry, D.; Stork, P. J. S.; Lazarovici, P.; Eiden, L. E. Signaling pathways for PC12 cell differentiation: Making the right connections. *Science* **2002**, *296*, 1648−1649.
(44) Arimura, N.; Kaibuchi, K. Neuronal polarity: from extracellular signals to intracellular mechanisms. *Nat. Rev. Neurosci.* **2007**, *8*, 194−205.
(45) Myers, J. P.; Gomez, T. M. Focal Adhesion Kinase Promotes Integrin Adhesion Dynamics Necessary for Chemotropic Turning of Nerve Growth Cones. *J. Neurosci.* **2011**, *31*, 13585−13595.
(46) Uebersax, L.; Mattotti, M.; Papaloizos, M.; Merkle, H.; Gander, B.; Meinel, L. Silk fibroin matrices for the controlled release of nerve growth factor (NGF). *Biomaterials* **2007**, *28*, 4449−4460.

https://doi.org/10.1021/acsomega.1c05117
ACS Omega 2021, 6, 33010−33017